

# Persistent near-tropical warmth on the Antarctic continent during the early Eocene epoch

Jörg Pross<sup>1,2</sup>, Lineth Contreras<sup>1</sup>, Peter K. Bijl<sup>3</sup>, David R. Greenwood<sup>4</sup>, Steven M. Bohaty<sup>5</sup>, Stefan Schouten<sup>6</sup>, James A. Bendle<sup>7</sup>, Ursula Röhl<sup>8</sup>, Lisa Tauxe<sup>9</sup>, J. Ian Raine<sup>10</sup>, Claire E. Huck<sup>11</sup>, Tina van de Flierdt<sup>11</sup>, Stewart S. R. Jamieson<sup>12</sup>, Catherine E. Stickley<sup>13</sup>, Bas van de Schootbrugge<sup>1</sup>, Carlota Escutia<sup>14</sup>, Henk Brinkhuis<sup>3</sup> & Integrated Ocean Drilling Program Expedition 318 Scientists\*

The warmest global climates of the past 65 million years occurred during the early Eocene epoch (about 55 to 48 million years ago), when the Equator-to-pole temperature gradients were much smaller than today<sup>1,2</sup> and atmospheric carbon dioxide levels were in excess of one thousand parts per million by volume<sup>3,4</sup>. Recently the early Eocene has received considerable interest because it may provide insight into the response of Earth's climate and biosphere to the high atmospheric carbon dioxide levels that are expected in the near future<sup>5</sup> as a consequence of unabated anthropogenic carbon emissions<sup>4,6</sup>. Climatic conditions of the early Eocene 'greenhouse world', however, are poorly constrained in critical regions, particularly Antarctica. Here we present a well-dated record of early Eocene climate on Antarctica from an ocean sediment core recovered off the Wilkes Land coast of East Antarctica. The information from biotic climate proxies (pollen and spores) and independent organic geochemical climate proxies (indices based on branched tetraether lipids) yields quantitative, seasonal temperature reconstructions for the early Eocene greenhouse world on Antarctica. We show that the climate in lowland settings along the Wilkes Land coast (at a palaeolatitude of about 70° south) supported the growth of highly diverse, near-tropical forests characterized by mesothermal to megathermal floral elements including palms and Bombacoideae. Notably, winters were extremely mild (warmer than 10 °C) and essentially frost-free despite polar darkness, which provides a critical new constraint for the validation of climate models and for understanding the response of high-latitude terrestrial ecosystems to increased carbon dioxide forcing.

The climate and ecosystem evolution on Antarctica before the onset of continental-scale glaciation at the Eocene/Oligocene transition (~33.9 Myr ago) is still poorly resolved owing to the obliteration or coverage of potential archives by the Antarctic ice sheet. Available data are primarily based on records from the Antarctic Peninsula, which are only partly representative of climate and ecosystem conditions on the Antarctic mainland<sup>7</sup>. Terrestrial proxy data generally indicate cool temperate conditions supporting a vegetation dominated by podocarpaceous conifers during the Palaeocene epoch (~65–56 Myr ago) and southern beech (*Nothofagus*) during the middle Eocene epoch (~49–37 Myr ago), followed by the final demise of angiosperm-dominated woodlands as a result of Cenozoic cooling and the development of the Antarctic cryosphere around Eocene/Oligocene boundary times<sup>8–10</sup>. This virtually makes the terrestrial realm of the high southern latitudes a climatic *terra incognita* for the peak warming phase of the Cenozoic greenhouse world.

We apply terrestrial palynology and palaeothermometry based on the methylation index of branched tetraethers (MBT) and the cyclization ratio of branched tetraethers (CBT) to a new sedimentary record from the Wilkes Land margin, East Antarctica, recovered by the Integrated Ocean Drilling Program (IODP Expedition 318 Site U1356; see ref. 11 and Fig. 1). These data sets provide the framework for a terrestrial climate reconstruction for the early Eocene of Antarctica. The record presented here comprises a succession of mid-shelfal sediments with excellent chronostratigraphic control (Supplementary Fig. 1), representing early Eocene (53.6–51.9 Myr ago) greenhouse conditions and, separated by a ~2 Myr hiatus, an

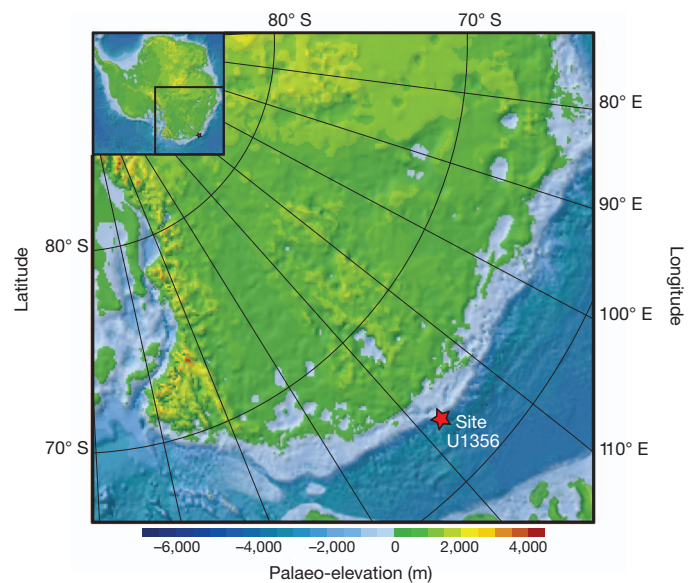


**Figure 1 | Site location and continental setting of Antarctica during early Eocene times.** Pre-glacial topographical reconstruction for Antarctica during Eocene–Oligocene times. Reconstructed elevations are used here to define minimum elevations for the early Eocene (Supplementary Information). The reconstruction indicates the likely presence of extensive lowlands along the Wilkes Land margin and higher-altitude settings in the hinterland, both of which represent the main catchment area for the terrestrial climate proxies (sporomorphs and biomarkers) studied at Site U1356. Palaeotopography after ref. 29; early Eocene coordinates obtained from the Ocean Drilling Stratigraphic Network after ref. 30.

<sup>1</sup>Paleoenvironmental Dynamics Group, Institute of Geosciences, Goethe University Frankfurt, Altenhöferallee 1, 60438 Frankfurt, Germany. <sup>2</sup>Biodiversity and Climate Research Centre, Senckenberganlage 25, 60325 Frankfurt, Germany. <sup>3</sup>Biomarine Sciences, Institute of Environmental Biology, Laboratory of Palaeobotany and Palynology, Utrecht University, Budapestlaan 4, 3584 CD Utrecht, The Netherlands. <sup>4</sup>Biology Department, Brandon University, 270 18th Street, Brandon, Manitoba R7A 6A9, Canada. <sup>5</sup>Ocean and Earth Science, National Oceanography Centre Southampton, University of Southampton, European Way, Southampton SO14 3ZH, UK. <sup>6</sup>Department of Marine Organic Biogeochemistry, NIOZ Royal Netherlands Institute of Sea Research, Post Office 59, 1790 AB Den Burg (Texel), The Netherlands. <sup>7</sup>Glasgow Molecular Organic Geochemistry Laboratory, School of Geographical and Earth Sciences, University of Glasgow, Glasgow G12 8QQ, UK. <sup>8</sup>MARUM – Center for Marine Environmental Sciences, University of Bremen, Leobener Straße, 28359 Bremen, Germany. <sup>9</sup>Scripps Institution of Oceanography, University of California, San Diego, La Jolla, California 92093, USA. <sup>10</sup>Department of Palaeontology, GNS Science, PO Box 30368, Lower Hutt 6009, New Zealand. <sup>11</sup>Imperial College London, Department of Earth Science and Engineering, South Kensington Campus, Exhibition Road, London SW7 2AZ, UK. <sup>12</sup>Department of Geography, Durham University, Science Laboratories, South Road, Durham DH1 3LE, UK. <sup>13</sup>Department of Geology, University of Tromsø, 9037 Tromsø, Norway. <sup>14</sup>Instituto Andaluz de Ciencias de la Tierra, Avenida de las Palmeras, 4 18100 Armilla (Granada), Spain.

\*Lists of participants and affiliations appear at the end of the paper.

interval of cooling presumed within the latest early Eocene to middle Eocene (49.3–46 Myr ago; here informally referred to as the ‘mid-Eocene’). Palynological and geochemical evidence independently supports the contention that the Wilkes Land sector of Antarctica is indeed the source region for the Eocene terrestrial palynomorphs and biomarkers present in the sediment core from Site U1356 (Supplementary Information).

Non-metric multidimensional scaling techniques show that the Eocene sporomorph assemblages at Site U1356 represent two main biomes (Fig. 2 and Supplementary Information). A highly diverse paratropical rainforest biome prevailed during the early Eocene, probably occupying the coastal lowlands of the Wilkes Land margin. This biome includes numerous mesothermal to megathermal taxa characteristic of modern subtropical to tropical settings in Australia, New Guinea and New Caledonia<sup>12</sup>. In addition to ferns and tree ferns (*Lygodium*, Cyatheaceae), it is characterized by the presence of palms (Arecaceae), Bombacoideae (Malvaceae), *Strasburgeria* (Strasburgeriaceae), *Beauprea* (Proteaceae), *Anacolsa* (Olacaceae) and *Spathiphyllum* (Araceae) (Fig. 2). Although these additional taxa occur only in low abundance, their presence is highly significant. Because they are pollinated by insects, their pollen dispersal in extant rainforests is generally restricted to less than 100 m (ref. 13). Hence, even low percentages of their pollen in the Site U1356 record indicate that these plants formed a substantial part of the Wilkes Land margin vegetation.

The palm and Bombacoideae pollen not only represent the southernmost documented occurrences for both taxa during the Eocene, but, importantly, imply that winter temperatures remained substantially above freezing. Extant palms occur naturally only in regions with a coldest-month mean temperature (CMMT) of  $\geq 5^{\circ}\text{C}$  (ref. 1). Because their cold-season temperature requirements increase further when palms grow under a high partial pressure of atmospheric  $\text{CO}_2$ , the CMMT implied by palms during the early Eocene greenhouse world was at least  $8^{\circ}\text{C}$  (ref. 14). Even warmer conditions are suggested by the record of Bombacoideae, which today occur where CMMT  $> 10^{\circ}\text{C}$ . Because even the most winter-hardy extant palms are severely

damaged by short-term freezing, with a series of consecutive years of unfavourable climate eventually being lethal<sup>15</sup>, winters must have been essentially frost-free.

Sporomorphs representing a lower-diversity temperate rainforest biome, with taxa characteristic of extant forests in montane settings of Australia, New Caledonia, New Guinea and New Zealand<sup>12</sup>, typically account for  $\sim 30\%$  of sporomorphs during the early Eocene. Characteristic taxa include *Nothofagus* (*fusca* type), Araucariaceae, Proteaceae and *Podocarpus*; mesothermal to megathermal, frost-sensitive taxa are consistently absent. Judging from its floral composition, this temperate rainforest biome occupied cooler environments of Wilkes Land located farther inland and/or at higher elevations, and therefore provides insight into the climate conditions deeper within the Antarctic continent. The coeval existence of a temperate rainforest biome in the hinterland and a paratropical rainforest in the lowlands of the Wilkes Land margin indicates a pronounced continental interior-to-coastal temperature gradient during the early Eocene.

A markedly different vegetation pattern is documented for the mid-Eocene time interval, with a strong expansion of the *Nothofagus*-dominated temperate rainforest biome and the near-extirpation of the paratropical rainforest biome; notably, the remainder of the latter biome is devoid of megathermal elements (Fig. 2). Hence, our data suggest that the temperate rainforest biome became dominant over the entire catchment area of Site U1356, also extending into the coastal regions, and that relict mesothermal components of the paratropical rainforest biome persisted only in localized pockets along the Wilkes Land margin. These shifts in dominance and floral composition indicate a strong cooling, which in light of the cold-season sensitivity of meso- and megathermal taxa was particularly pronounced in winter temperatures, and a strong weakening of the temperature gradient between coastal and montane regions of the Wilkes Land margin.

To quantify further the sporomorph-derived palaeoclimatic information, we carried out bioclimatic analyses using the nearest living relative concept<sup>16</sup> to reconstruct the mean annual temperature (MAT), the mean winter and summer temperatures (MWT and MST)

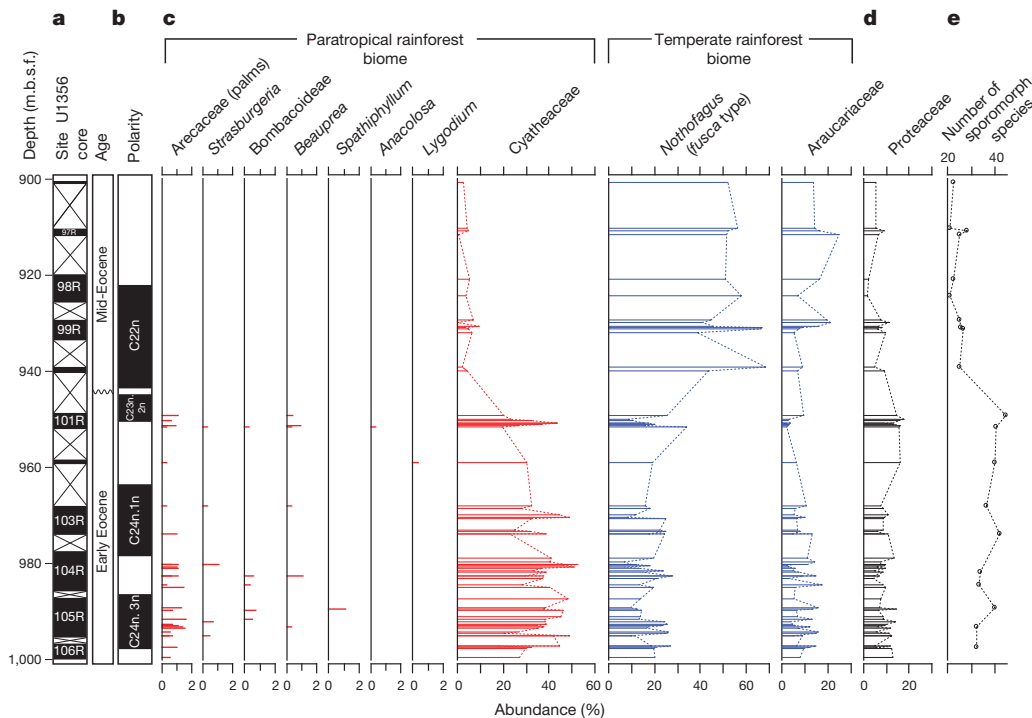


**Figure 2** | Data from Site U1356 for the early Eocene to mid-Eocene. **a**, Core recovery. m.b.s.f., metres below sea floor. **b**, Geological age<sup>11</sup>. **c**, Relative abundances of selected sporomorphs representative of the paratropical and temperate rainforest biomes. **d**, Relative abundances of Proteaceae pollen. Data

based on samples with counts of  $\geq 90$  specimens. **e**, Number of sporomorph species rarefied at 280 grains. The number of sporomorph species from the early Eocene is significantly higher than that from the mid-Eocene (Mann-Whitney test,  $P < 0.000005$ ).

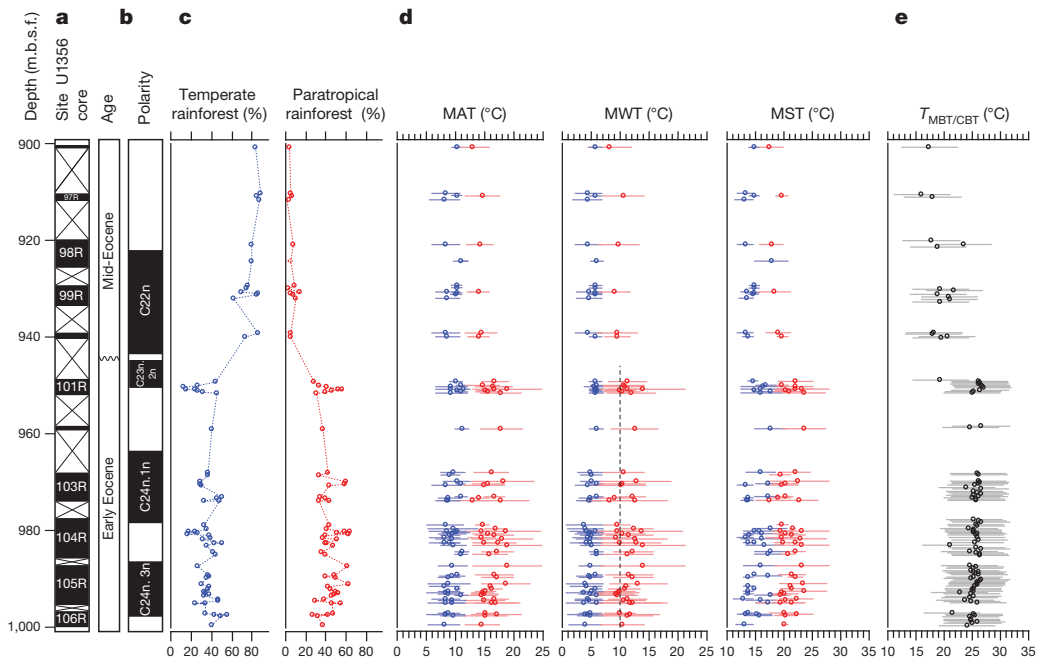


**Figure 3 | Climate reconstruction for the Wilkes Land sector of Antarctica during the early and mid-Eocene derived from Site U1356. a, Core recovery. b, Geological age<sup>11</sup>. c, Relative abundances of sporomorphs representing the temperate and paratropical rainforest biomes. d, Estimates of MAT, MWT and MST for the temperate (blue) and paratropical (red) rainforest biomes, based on the methodology of ref. 16. Error bars represent the minimum and maximum estimates determined using that method. The vertical dashed line**

(Fig. 3), and the mean annual precipitation (Supplementary Fig. 5). These results were critically assessed through a comparison with reconstructions using a different methodology that also relies on the nearest living relative concept (the coexistence approach of ref. 17; see Supplementary Information). Because the two recognized biomes represent distinct environments with different climatic conditions, our approach allows a spatiotemporally differentiated view of the climate evolution of Wilkes Land from early Eocene peak warmth through the onset of mid-Eocene cooling. Our temperature estimates for the paratropical rainforest biome show that climate along the Wilkes Land margin was generally warm until at least 51.9 Myr ago. Most samples indicate temperatures of  $16 \pm 5^\circ\text{C}$  for MAT,  $11 \pm 5^\circ\text{C}$  for MWT and  $21 \pm 5^\circ\text{C}$  for MST, although a small number also yield colder or warmer values (Fig. 3). A markedly cooler climate emerges for the temperate rainforest biome, in particular for MAT and MWT, for which most samples yield values of  $9 \pm 3^\circ\text{C}$  and  $5 \pm 2^\circ\text{C}$ , respectively. For MST, the data show a strong scatter between  $14 \pm 1^\circ\text{C}$  and  $18 \pm 3^\circ\text{C}$ , and the values overlap partly with those for the paratropical rainforest biome. For both biomes, the mean annual precipitation was persistently more than  $100 \text{ cm yr}^{-1}$  (Supplementary Information).

For the mid-Eocene interval, our reconstructions based on the relicts of the paratropical rainforest biome suggest a pronounced cooling, although this trend is partly within the error limits of the data. The estimated MAT is  $14 \pm 3^\circ\text{C}$ , which represents a decline of  $\sim 2^\circ\text{C}$  from the early Eocene. Our data also indicate a decline in MWT and MST, although these trends are again within the error limits. Temperatures reconstructed for the temperate rainforest biome are comparable to those from the early Eocene, which is consistent with there being no major changes in the composition of this biome between both intervals.

Independent support for a warm terrestrial climate during the early Eocene and marked cooling during the mid-Eocene comes from our MBT/CBT palaeothermometry data (Fig. 3). Soil temperatures of  $\sim 24\text{--}27^\circ\text{C}$  are estimated for the early Eocene, and  $\sim 17\text{--}20^\circ\text{C}$  for the mid-Eocene. These temperatures fall close to the MSTs derived for the paratropical rainforest biome. This suggests that the branched

marks the minimum requirements of Bombacoideae for the mean temperature of the coldest month. e, Temperatures derived from the MBT/CBT index, with horizontal error bars indicating the calibration standard error ( $\pm 5^\circ\text{C}$ ). This error refers to absolute temperature estimates across all environmental settings of the modern calibration; thus, the error of the within-record variation is much smaller. Relative sporomorph abundances and sporomorph-based climate estimates are based on samples with counts of  $\geq 90$  specimens.

tetraethers in Site U1356 sediments originated from coastal lowland soils of the Wilkes Land sector of Antarctica and could imply a bias of the MBT/CBT proxy towards summer temperatures, although such a bias has not been observed in modern mid-latitude climates (Supplementary Information).

Our data, which provide continental temperature reconstructions for the high southern latitudes during the early Eocene greenhouse world, show that paratropical conditions persisted in the lowlands of the Wilkes Land margin of Antarctica from at least 53.9 to 51.9 Myr ago. Notably, our estimates yield a constraint on Antarctic winter temperatures during peak greenhouse conditions. The CMMT and MWT estimates of  $\geq 10^\circ\text{C}$  and  $11 \pm 5^\circ\text{C}$ , respectively, compare favourably with deep-water temperatures of  $\sim 11^\circ\text{C}$  in the marine realm at this time<sup>6,18</sup>. Because early Eocene deep waters were sourced from downwelling surface waters in the high southern latitudes off Antarctica<sup>19</sup>, winter temperatures in these regions cannot have dropped much below  $11^\circ\text{C}$ . Although our MWT estimates are not representative of the Antarctic continent as a whole, they bear implications for the current debates on the general ability of climate models to reproduce extreme greenhouse conditions and the response of polar ecosystems to increased  $\text{CO}_2$  forcing.

When run with conservative estimates of atmospheric  $\text{CO}_2$  levels for the early Eocene, fully coupled climate models yield high-latitude terrestrial winter temperatures considerably below freezing<sup>20</sup>, and they produce warm (that is, above-freezing) winters in the terrestrial high latitudes only when radiative forcing is strongly enhanced<sup>21</sup>. Hence, our winter temperatures for Wilkes Land provide a critical reference point for understanding the climate dynamics of the early Eocene greenhouse world. They are in remarkably close agreement with simulated MWTs for the Wilkes Land region when radiative forcings equivalent to 2,240 p.p.m.v. and 4,480 p.p.m.v.  $\text{CO}_2$  are applied (ref. 21), suggesting that enhancing radiative forcing in models may help resolve the persistent data–model mismatch. However, factors other than extremely high atmospheric greenhouse gas forcing may have contributed to the winter warmth along the Wilkes Land sector of Antarctica. They



include winter cloud radiative forcing over high-latitude land masses<sup>22</sup>, possibly connected to high ocean-to-land moisture transport<sup>23</sup>. Our precipitation estimates (Supplementary Fig. 5) and the presence of rainforest biomes consistently suggest high moisture availability throughout the year, thus lending support for this mechanism being in operation in the Wilkes Land sector of Antarctica. A high moisture flux from the ocean was facilitated by the presence of extremely warm surface waters in the Australo-Antarctic gulf, resulting from the sub-tropically derived, clockwise-flowing proto-Leeuwin current<sup>24</sup>. Warm surface waters off Wilkes Land are documented by mass occurrences of the subtropical dinoflagellate cyst *Apectodinium*<sup>11</sup>.

Our data also provide new insights into the physiological ecology of high-latitude forests, which are subject to seasonally extreme changes in light levels. The ~50 days of polar darkness on the Wilkes Land margin poses severe constraints on the plants' carbon gain by photosynthesis and carbon loss by respiration. Because carbon loss by respiration typically increases with temperature<sup>25</sup>, it has been argued that polar winters must have been cool rather than warm<sup>26</sup>. Our MBT/CBT temperature data, which under the most conservative (that is, 'coldest') assumption represent MST, are typically between 24 and 27 °C for the early Eocene (Fig. 3). They are similar to, although possibly slightly warmer than, the terrestrial MST predicted by climate models using high radiative forcing (20–25 °C; ref. 21). Over a wide range of CO<sub>2</sub> forcing, the models yield a temperature seasonality of the order of 10 °C, thus suggesting a MWT of 10–15 °C. This evidence, which is strictly independent of our vegetation-based climate reconstructions, contradicts the scenario of cold winters on Wilkes Land, therefore suggesting that respiration losses under a highly seasonal polar light regime were compensated for by a factor other than temperature. We suggest that the high atmospheric CO<sub>2</sub> levels of the early Eocene greenhouse climate were a decisive factor in the physiological ecology of high-latitude forests, most probably through causing a reduction in carbon respiration during the polar winter<sup>27</sup> and an increase in photosynthetic carbon gain during the growing season<sup>28</sup>.

Our new data from the peak early Eocene greenhouse world indicate that a highly diverse forest vegetation containing evergreen elements can successfully colonize high-latitude, warm winter environments when atmospheric CO<sub>2</sub> levels are high. Depending on the thresholds in atmospheric CO<sub>2</sub> required by such plants, the duration of polar winters and the temperatures at which such forcing factors become significant, these results have important implications for the composition of high-latitude terrestrial ecosystems in a future anthropogenic greenhouse world with high atmospheric CO<sub>2</sub> levels and drastic polar amplification of warming.

## METHODS SUMMARY

**Palynology.** Between 10 and 15 g of sediment was processed per sample. The dried sediment was weighed and spiked with *Lycopodium* spores to facilitate the calculation of absolute palynomorph abundances. Chemical processing comprised treatment with 30% HCl and 38% HF for carbonate and silica removal, respectively. Ultrasonication was used to disintegrate palynodebris. Residues were sieved over a 10-µm mesh and mounted on microscope slides, which were analysed at ×200 and ×1,000 magnification. A detailed, step-by-step processing protocol is given in Supplementary Information.

**Sporomorph-based climate reconstructions.** Bioclimatic analyses were carried out following ref. 16, but with data sources including Southern Hemisphere taxa, allowing the development of climatic profiles for each taxon as described in Supplementary Information. The results of the bioclimatic analyses were critically assessed through the application of the coexistence approach<sup>17</sup> to the data set using the same underlying database. Supplementary Table 1 lists all taxa that were evaluated through the bioclimatic analyses and the coexistence approach, their botanical affinity and the nearest living relatives used in the analyses.

**Organic geochemistry.** For MBT/CBT analyses, freeze-dried, powdered samples were extracted with an accelerated solvent extractor using a 9:1 (v/v) dichloromethane (DCM):methanol solvent mixture. The obtained extracts were separated over an activated Al<sub>2</sub>O<sub>3</sub> column, using 9:1 (v/v) hexane:DCM, 1:1 (v/v) hexane: DCM, 1:1 (v/v) ethylacetate:DCM and 1:1 (v/v) DCM:methanol, into apolar, ketone, ethylacetate and polar fractions, respectively. The polar fractions

containing the branched tetraether lipids were analysed by HPLC/APCI-MS (high-performance liquid chromatography/atmospheric pressure chemical ionization mass spectrometry) using an Agilent 1100 LC/MSD SL. MBT/CBT indices were calculated and converted into temperature estimates as described in Supplementary Information.

Received 28 February; accepted 8 June 2012.

- Greenwood, D. R. & Wing, S. L. Eocene continental climates and latitudinal temperature gradients. *Geology* **23**, 1044–1048 (1995).
- Bijl, P. K. *et al.* Early Palaeogene temperature evolution of the southwest Pacific Ocean. *Nature* **461**, 776–779 (2009).
- Yapp, C. J. Fe(CO<sub>3</sub>)OH in goethite from a mid-latitude North American oxisol: estimate of atmospheric CO<sub>2</sub> concentration in the Early Eocene "climatic optimum". *Geochim. Cosmochim. Acta* **68**, 935–947 (2004).
- Beerling, D. J. & Royer, D. L. Convergent Cenozoic CO<sub>2</sub> history. *Nat. Geosci.* **4**, 418–420 (2011).
- Meinshausen, M. *et al.* The RCP greenhouse gas concentrations and their extensions from 1765 to 2300. *Clim. Change* **109**, 213–241 (2011).
- Zachos, J. C., Dickens, G. R. & Zeebe, R. E. An early Cenozoic perspective on greenhouse warming and carbon-cycle dynamics. *Nature* **451**, 279–283 (2008).
- Anderson, J. B. *et al.* Progressive Cenozoic cooling and the demise of Antarctica's last refugium. *Proc. Natl Acad. Sci. USA* **108**, 11356–11360 (2011).
- Francis, J. E. Antarctic palaeobotany: clues to climate change. *Terra Antarctica* **3**, 135–140 (1996).
- Poole, I., Cantrill, D. & Utescher, T. A multi-proxy approach to determine Antarctic terrestrial palaeoclimate during the Late Cretaceous and Early Tertiary. *Palaeogeogr. Palaeoclimatol. Palaeoecol.* **222**, 95–121 (2005).
- Truswell, E. M. & Macphail, M. K. Polar forests on the edge of extinction: what does the fossil spore and pollen evidence from East Antarctica say? *Aust. Syst. Bot.* **22**, 57–106 (2009).
- Expedition 318 Scientists in *Proc. IODP*, Vol. 318 (eds Escutia, C., Brinkhuis, H., Klaus, A., and the Expedition 318 Scientists) (Integrated Ocean Drilling Program Management International, Inc., 2011).
- Kershaw, A. P. in *Vegetation History* (eds Huntley, B. & Webb, T.) 237–306 (Kluwer, 1988).
- Bush, M. B. & Rivera, R. Pollen dispersal and representation in a neotropical rain forest. *Glob. Ecol. Biogeogr.* **7**, 379–392 (1998).
- Royer, D. L., Osborne, C. P. & Beerling, D. J. High CO<sub>2</sub> increases the freezing sensitivity of plants: implications for paleoclimatic reconstructions from fossil floras. *Geology* **30**, 963–966 (2002).
- Larcher, W. & Winter, A. Frost susceptibility of palms: experimental data and their interpretation. *Principes* **25**, 143–152 (1981).
- Greenwood, D. R., Archibald, S. B., Mathewes, R. W. & Moss, P. T. Fossil biotas from the Okanagan Highlands, southern British Columbia and northeastern Washington State: climates and ecosystems across an Eocene landscape. *Can. J. Earth Sci.* **42**, 167–185 (2005).
- Mosbrugger, V. & Utescher, T. The coexistence approach – a method for quantitative reconstructions of Tertiary terrestrial palaeoclimate data using plant fossils. *Palaeogeogr. Palaeoclimatol. Palaeoecol.* **134**, 61–86 (1997).
- Lear, C. H., Elderfield, H. & Wilson, P. A. Cenozoic deep-sea temperatures and global ice volumes from Mg/Ca in benthic foraminiferal calcite. *Science* **287**, 269–272 (2000).
- Thomas, D. J., Bralower, T. J. & Jones, C. E. Neodymium isotopic reconstruction of late Paleocene-early Eocene thermohaline circulation. *Earth Planet. Sci. Lett.* **209**, 309–322 (2003).
- Shellito, C. J., Sloan, L. C. & Huber, M. Climate model sensitivity to atmospheric CO<sub>2</sub> levels in the Early-Middle Paleogene. *Palaeogeogr. Palaeoclimatol. Palaeoecol.* **193**, 113–123 (2003).
- Huber, M. & Caballero, R. The early Eocene equable climate problem revisited. *Clim. Past* **7**, 603–633 (2011).
- Abbot, D. S., Huber, M., Bousquet, G. & Walker, C. C. High-CO<sub>2</sub> cloud radiative forcing feedback over both land and ocean in a global climate model. *Geophys. Res. Lett.* **36** (2009).
- Abbot, D. S. & Tziperman, E. Sea ice, high-latitude convection, and equable climates. *Geophys. Res. Lett.* **35** (2008).
- Huber, M. *et al.* Eocene circulation of the Southern Ocean: was Antarctica kept warm by subtropical waters? *Paleoceanography* **19** (2004).
- Tjoelker, M. G., Oleksyn, J. & Reich, P. B. Modelling respiration of vegetation: evidence for a general temperature-dependent Q<sub>10</sub>. *Glob. Change Biol.* **7**, 223–230 (2001).
- Read, J. & Francis, J. Responses of some Southern Hemisphere tree species to a prolonged dark period and their implications for high-latitude Cretaceous and Tertiary floras. *Palaeogeogr. Palaeoclimatol. Palaeoecol.* **99**, 271–290 (1992).
- Beerling, D. J. & Osborne, C. P. Physiological ecology of Mesozoic polar forests in a high CO<sub>2</sub> environment. *Ann. Bot. (Lond.)* **89**, 329–339 (2002).
- DeLucia, E. H. *et al.* Net primary production of a forest ecosystem with experimental CO<sub>2</sub> enrichment. *Science* **284**, 1177–1179 (1999).
- Wilson, D. S. *et al.* Antarctic topography at the Eocene-Oligocene boundary. *Palaeogeogr. Palaeoclimatol. Palaeoecol.* **335–336**, 24–34 (2011).
- Hay, W. W. *et al.* Alternative global Cretaceous paleogeography. *Spec. Publ. Geol. Soc. Am.* **332**, 1–47 (1999).

Supplementary Information is linked to the online version of the paper at [www.nature.com/nature](http://www.nature.com/nature).

**Acknowledgements** This research used samples and data provided by the Integrated Ocean Drilling Program (IODP). The IODP is sponsored by the US National Science Foundation and participating countries under the management of Joint Oceanographic Institutions, Inc. Financial support for this research was provided by the German Research Foundation, to J.P. (grant PR 651/10) and U.R. (grant RO 1113/6); the Biodiversity and Climate Research Center of the Hessian Initiative for Scientific and Economic Excellence, to J.P.; the Netherlands Organisation for Scientific Research, to H.B. and S.S. (VICI grant); the Natural Sciences and Engineering Research Council of Canada, to D.R.G. (grant DG 311934); the Natural Environment Research Council, to S.M.B. (grant Ne/J019801/1), J.A.B. (grant Ne/I00646X/1) and T.v.d.F. (grant Ne/I006257/1); the US National Science Foundation, to L.T. (grant OCE 1058858); and the New Zealand Ministry of Science and Innovation, to J.I.R. We thank J. Francis, S. Gollner and M. Huber for discussions, and B. Coles, E. Hopmans, K. Kreissig, A. Mets, J. Ossebaer, B. Schminke, J. Treehorn and N. Welters for technical support.

**Author Contributions** J.P., H.B. and S.S. designed the research. L.C., J.P. and J.I.R. analysed the sporomorphs, D.R.G. and L.C. conducted the quantitative climate reconstructions, and P.K.B. and S.S. carried out the MBT/CBT analyses. All authors contributed to the interpretation of the data. J.P. wrote the paper with input from all authors.

**Author Information** Reprints and permissions information is available at [www.nature.com/reprints](http://www.nature.com/reprints). The authors declare no competing financial interests. Readers are welcome to comment on the online version of this article at [www.nature.com/nature](http://www.nature.com/nature). Correspondence and requests for materials should be addressed to J.P. ([joerg.pross@em.uni-frankfurt.de](mailto:joerg.pross@em.uni-frankfurt.de)).

**Integrated Ocean Drilling Program Expedition 318 Scientists** Henk Brinkhuis<sup>1</sup>, Carlota Escutia Dotti<sup>2</sup>, Adam Klaus<sup>3</sup>, Annick Fehr<sup>4</sup>, Trevor Williams<sup>5</sup>, James A. P. Bendle<sup>6</sup>, Peter K. Bijl<sup>1</sup>, Steven M. Bohaty<sup>7</sup>, Stephanie A. Car<sup>8</sup>, Robert B. Dunbar<sup>9</sup>, Jhon J. González<sup>2</sup>, Travis G. Hayden<sup>10</sup>, Masao Iwai<sup>11</sup>, Francisco J. Jimenez-Espejo<sup>12†</sup>, Kota Katsuki<sup>13</sup>, Gee Soo Kong<sup>14</sup>, Robert M. McKay<sup>15</sup>, Mutsumi Nakai<sup>16</sup>, Matthew P. Olney<sup>17</sup>, Sandra Passchier<sup>18</sup>, Stephen F. Pekar<sup>19</sup>, Jörg Pross<sup>20,21</sup>, Christina R. Riesselman<sup>9†</sup>, Ursula Röhl<sup>22</sup>, Toyosaburo Sakai<sup>23</sup>, Prakash K. Shrivastava<sup>24</sup>, Catherine E. Stickley<sup>25</sup>, Saiko Sugisaki<sup>26†</sup>, Lisa Tauxe<sup>27</sup>, Shouting Tuo<sup>28</sup>, Tina van de Flierdt<sup>29</sup>, Kevin Welsh<sup>30</sup> & Masako Yamane<sup>31</sup>

Affiliations for participants: <sup>1</sup>Biomarine Sciences, Institute of Environmental Biology, Laboratory of Palaeobotany and Palynology, Utrecht University, Budapestlaan 4, 3584 CD Utrecht, The Netherlands. <sup>2</sup>Instituto Andaluz de Ciencias de la Tierra, CSIC-Universidad de Granada, Campus de Fuentenueva s/n, 18002 Granada, Spain. <sup>3</sup>United States Implementing Organization, Integrated Ocean Drilling Program, Texas A&M University, 1000 Discovery Drive, College Station, Texas 77845, USA. <sup>4</sup>Aachen University, Institute for

Applied Geophysics and Geothermal Energy, Mathieustraße 6, D-52074 Aachen, Germany. <sup>5</sup>Borehole Research Group, Lamont-Doherty Earth Observatory of Columbia University, PO Box 1000, 61 Route 9W, Palisades, New York 10964, USA. <sup>6</sup>Geographical and Earth Sciences, University of Glasgow, G128QQ Glasgow, UK. <sup>7</sup>Ocean and Earth Science, National Oceanography Centre Southampton, University of Southampton, European Way, SO14 3ZH Southampton, UK. <sup>8</sup>Department of Chemistry and Geochemistry, Colorado School of Mines, 1500 Illinois Street, Golden, Colorado 80401, USA. <sup>9</sup>Department of Environmental Earth System Science, Stanford University, 325 Braun Hall, Building 320, Stanford, California 94305-2115, USA. <sup>10</sup>Department of Geology, Western Michigan University, 1187 Rood Hall, 1903 West Michigan Avenue, Kalamazoo, Michigan 49008, USA. <sup>11</sup>Department of Natural Science, Kochi University, 2-5-1 Akebono-cho, Kochi 780-8520, Japan. <sup>12</sup>Institute for Research on Earth Evolution, Japan Agency for Marine-Earth Science and Technology, Natsushima-cho 2-15, Yokosuka 237-0061, Japan. <sup>13</sup>Marine Center for Advanced Core Research, Kochi University, B200 Monobe, Nankoku, Kochi 783-8502, Japan. <sup>14</sup>Petroleum and Marine Research Division, Korea Institute of Geoscience and Mineral Resources, 30 Gajeong-dong, Yuseong-gu, Daejeon 305-350, Republic of Korea. <sup>15</sup>Antarctic Research Centre, Victoria University of Wellington, PO Box 600, Wellington 6140, New Zealand. <sup>16</sup>Education Department, Daito Bunka University, 1-9-1 Takashima-daira, Itabashi-ku, Tokyo 175-8571, Japan. <sup>17</sup>Department of Geology, University of South Florida, Tampa, 4202 East Fowler Avenue, SCA 528, Tampa, Florida 33620, USA. <sup>18</sup>Earth and Environmental Studies, Montclair State University, 252 Mallory Hall, 1 Normal Avenue, Montclair, New Jersey 07043, USA. <sup>19</sup>School of Earth and Environmental Sciences, Queens College, 65-30 Kissena Boulevard, Flushing, New York 11367, USA. <sup>20</sup>Paleoenvironmental Dynamics Group, Institute of Geosciences, Goethe University Frankfurt, Altenhöferallee 1, 60438 Frankfurt, Germany. <sup>21</sup>Biodiversity and Climate Research Centre, Senckenberganlage 25, 60325 Frankfurt, Germany. <sup>22</sup>MARUM – Center for Marine Environmental Sciences, University of Bremen, Leobener Straße, 28359 Bremen, Germany. <sup>23</sup>Department of Geology, Utsunomiya University, 350 Mine-Machi, Utsunomiya 321-8505, Japan. <sup>24</sup>Antarctica Division, Geological Survey of India, NH5P, NIT, Faridabad 121001, Harlyana, India. <sup>25</sup>Department of Geology, Universitet i Tromsø, N-9037 Tromsø, Norway. <sup>26</sup>Department of Polar Science, Graduate University of Advanced Study, 10-3 Midori-cho, Tachikawa City, Tokyo 190-8518, Japan. <sup>27</sup>Scripps Institution of Oceanography, University of California, San Diego, La Jolla, California 92093-0220, USA. <sup>28</sup>School of Ocean and Earth Science, Tongji University, 1239 Spring Road, Shanghai 200092, China. <sup>29</sup>Department of Earth Science and Engineering, Imperial College London, London SW7 2AZ, UK. <sup>30</sup>School of Earth Sciences, University of Queensland, St Lucia, Brisbane, Queensland 4072, Australia. <sup>31</sup>Earth and Planetary Science, University of Tokyo, 7-3-1 Hongo, Bunkyo-ku, Tokyo 113-0033, Japan. †Present addresses: Instituto Andaluz de Ciencias de la Tierra, CSIC-Universidad de Granada, Armilla, 18100 Granada, Spain (F.J.J.-E.); US Geological Survey, Eastern Geology and Paleoclimate Science Center, 926A National Center, Reston, Virginia 20192, USA (C.R.R.); Japan Agency for Marine-Earth Science and Technology, Frontier Building 4F, 2-15 Natsushima-cho, Yokosuka City, Kanagawa 237-0061, Japan (S.S.).